energy&fuels

pubs.acs.org/EF

Article

Electrochemical Coproduction of Hydrogen, Oxygen, Sodium Hydroxide, and Hydrochloric Acid from Brines via Direct Electrosynthesis with Chlorine Suppression

Published as part of Energy & Fuels virtual special issue "Celebrating Women in Energy Research".

Minkyeong Kim, Peilong Lu, Prince Ochonma, and Greeshma Gadikota*

Cite This: *Energy Fuels* 2024, 38, 15812−15822

Read Online

ACCESS | Metrics & More | Article Recommendations | Supporting Information

ABSTRACT: Hydrogen production is of growing interest as a low-carbon energy carrier. While technologies to produce H_2 via steam methane reforming and water electrolysis remain well developed, the use of brine electrolysis is gaining increasing attention due to the feasibility of producing multiple high-value coproducts, including acids, bases, and O_2. However, the conventional method for producing acid and base simultaneously using bipolar membrane electrodialysis (BMED) consumes significant energy and has a complex process configuration. Additionally, it is important to suppress Cl_2 gas evolution and produce HCl instead during brine electrolysis. This study investigates the performance and economic viability of three different brine electrolysis systems: direct electrosynthesis (DE) without a bipolar membrane, anion exchange membrane (AEM), and cation exchange membrane (CEM) systems, using a new manganese−molybdenum-coated titanium (MnMo/Ti) electrode that suppresses Cl_2 gas evolution. Results demonstrate that the DE-MnMo/Ti electrode system produced 0.005 mol of H_2, 0.0041 mol of O_2, 0.37 M NaOH, and 0.2 M HCl (~98% purity). Compared to pure water electrolysis, brine electrolysis offers higher economic potential due to the production of value-added products, such as O_2, NaOH, and HCl. The revenue generated per year using the proposed approach is 4 times higher than that of alkaline electrolysis using pure water, even though H_2 yields are lower compared to those of water electrolysis. By unlocking the feasibility of harnessing low value brines for brine electrolysis, the energy needs associated with producing fresh water via energy-intensive desalination processes are circumvented. Therefore, this study highlights the potential for brine electrolysis with the DE-MnMo/Ti electrode system as an economically viable and environmentally sustainable route for producing H_2, NaOH, HCl, and O_2.

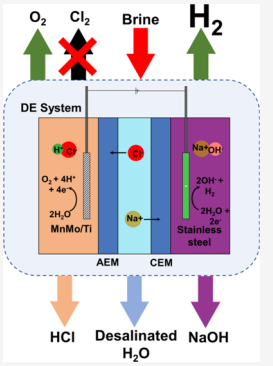

INTRODUCTION

The growing interest in harnessing H_2 as a clean energy carrier has motivated significant advances in technologies, such as steam methane reforming (SMR) and water electrolysis. However, H_2 production via SMR is accompanied by CO_2 emissions, which need to be captured and stored.[1] Managing CO_2 during or after H_2 production from carbon bearing feedstocks remains challenging, despite the progress that has been made.[2−5] Alternatively, water electrolysis is a promising pathway for carbon-free H_2 production; however, fresh water needed for water electrolysis requires energy-intensive desalination or extensive wastewater treatment.[6] These challenges motivate advances in harnessing alternate resources that cogenerate other high-value products alongside H_2 with reduced environmental impacts compared to conventional H_2 production technologies. Unlocking the use of natural brines (as in the case of seawater) or produced brines resulting from processes, such as desalination,[7] can potentially limit (a) CO_2 emissions compared to existing processes, (b) the need for freshwater supply, and (c) the release of brines into water bodies, which can be harmful to marine life.[8] Motivated by these challenges, this study aims to develop brine electrolysis approaches for coproducing H_2 along with other high-value products.[9] Further, by coupling the proposed technology with renewable energy sources, a more sustainable H_2 production can be achieved (Figure S1).

One approach for brine management involves the use of bipolar membrane electrodialysis (BMED). BMED is a process that couples electrodialysis with bipolar membranes and has been reported extensively to produce HCl and NaOH from brine.[10] However, there has been limited information on H_2 production in these systems (see Table 1). BMED studies have primarily sought to improve acid and base concentrations and reduce energy consumption. Proposed methods include coupling electrodialysis with evaporation to increase NaOH concentration and determining the optimal volume ratio of acid, base, and salt for brine electrolysis.[11,12] Most recently, there has

Received: February 25, 2024
Revised: July 14, 2024
Accepted: July 15, 2024
Published: July 30, 2024

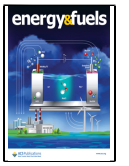

Table 1. Summary of the Key Studies Conducted on the Electrochemical Conversion of Brine to Acids, Bases, and H_2[a]

system	feed conc. (M)	current density (mA/cm^2)	current efficiency (%)	max. base conc. (M)	max. acid conc. (M)	energy consumed (kWh/kg)	Cl_2 suppression	produced H_2 (mol)	ref
DE	NaCl, 0.86	90	acid 20 base 36	NaOH, 0.37	HCl, 0.2	NaOH, 3.6	yes (anode: Ti coated with MnMo)	0.005	this work
DE	NaCl, 0.86	90	acid 11 base 28	NaOH, 0.63	HCl, 0.25	NaOH, 2.2	no (anode: Pt)	0.017	this work
DE	NaCl, 0.6	25	acid 65 base 88	NaOH, 0.22	HCl, 0.29	–	yes (anode: Ti coated with MnMo)	–	16
DE	K_2SO_4, 0.5	10	–	KOH, –	H_2SO_4, –	–	–	–	32
BMED	NaCl, 1	100	–	NaOH, 3.65	HCl, –	NaOH, 22.6	–	–	11
BMED	Wastewater	40	acid 55.2 base 50.2	NaOH, 1.56	H_2SO_4, 0.97	NaOH, 3.98	–	–	12
BMED	NaCl, 0.5	50	41–59	NaOH, 3.4	HCl, 2.3	NaOH, 1.5–1.9	–	–	38
BMED	NaCl, 1	100	–	NaOH, 3.6	HCl, 3.3	HCl, 43.5	–	–	27
BMED	NaCl, 1.3	3.67 V	50–53	NaOH, 1.75	HCl, 1.75	–	–	–	39
BMED	NaCl, 1.7–3.4	30–40	55–58	NaOH, 2	HCl, 2	NaOH, 1.7–3.6	–	–	29
BMED	NaCl, 2.0	30	acid 31–84 base 40–89	NaOH, 1.31	HCl, 1.18	NaOH, 1.14–2.74	–	–	18
BMED	NaCl, 2.0	10	52.7–83.6	NaOH, 0.93	HCl, 0.94	NaOH, 1.61–2.34	–	–	40
RE	NaCl, 0.017/0.6	0.02–1.4 V	–	–	–	H_2, 0.6–39	–	–	14
membraneless	seawater	1 V	–	NaOH, –	HCl, –	–	no (platinized carbon foam electrodes)	–	17

[a]The hyphen (–) is used when information is missing or not applicable.

been growing interest in reverse electrodialysis (RED), which utilizes two different salinity solutions to generate electric power, and can be adapted for hydrogen production.[13,14] However, an increase in acidic catholyte or alkaline anolyte concentration results in a corresponding increase in current density, which could reduce counterion diffusion.[13] Alternatively, direct electrosynthesis (DE) is another approach that avoids issues related to counterion-induced current density increase and also uses a relatively less number of membranes (Figure 1a).[9] Direct electrosynthesis utilizes electrolysis and selective ion transport for the concurrent production of HCl and NaOH, with O_2 and H_2 being produced at the anode and cathode, respectively. Electrodialysis, however, primarily aims to produce acid and base solutions only through the transport of salt ions. Moreover, DE systems avoid the relatively complex configuration design, high material requirements, and the need for multiple membranes associated with RED or BMED systems.[9,15] Several studies have shown the efficacy of the DE systems in reducing the energy requirements for brine electrolysis; however, finding a stable oxygen evolution reaction (OER) catalyst with high selectivity over chlorine evolution reaction (CER) remains a challenge. Only a few studies have reported Cl_2 suppression using DE systems. For example, Lin and co-workers inhibited Cl_2 gas evolution by using a $Mn_{0.84}Mo_{0.16}O_{0.23}$-coated titanium electrode in DE, although the resulting NaOH concentration was low and energy consumption data were not provided.[16] Badjatya and co-workers produced NaOH and HCl without a membrane and generated $Mg(OH)_2$ as a feedstock for cement production, but information on the concentration of NaOH, HCl, and H_2 produced, or whether Cl_2 formation was inhibited, is not available.[17] The need to suppress chlorine gas evolution distinguishes DE technology from the chloralkali industry, which aims to produce Cl_2. On the contrary, this study focuses on investigating the efficacy of MnMo/Ti anodes for suppressing Cl_2 gas evolution while coproducing H_2, O_2, NaOH, and HCl via direct electrosynthesis (DE) of brines.

Despite the several key advantages associated with the use of DE systems, several outstanding questions are yet to be addressed, such as (a) How can we utilize selective electrode materials such as MnMo on Ti to achieve higher asymmetric OER vs CER selectivity for the suppression of Cl_2 gas evolution in DE systems? (b) What is the influence of Cl_2 gas suppression on the corresponding formation of sodium hydroxide, hydrochloric acid, H_2, and O_2? (c) How does the coproduction of multiple high-value products along with the associated energy needs influence the overall economic potential of the direct electrosynthesis of brines? Addressing these questions will unlock new possibilities in the cogeneration of H_2 coupled with the generation of multiple high-value products via direct electrosynthesis of brine.

MATERIALS AND METHODS

Chemicals. The synthetic brines used in this study were prepared using sodium chloride (NaCl, ≥99%, Sigma-Aldrich). Acid and base adjustments were made using hydrochloric acid (HCl, 12.1 M, Fisher Chemical) and sodium hydroxide (NaOH, Lab grade, Fisher bioreagents). The catalysts were synthesized using manganese sulfate ($MnSO_4$, ≥98%, Chemworld), sodium molybdate dihydrate ($Na_2MoO_4{\cdot}2H_2O$, ≥99.5%, Sigma-Aldrich), ascorbic acid ($C_6H_8O_6$, 100%, Cole-Parmer), and potassium iodide (KI, ≥99%, Sigma-Aldrich). Deionized water (18.2 MΩ·cm, Millipore) was used throughout the experiments.

Experimental Approach. Three systems, including direct electrosynthesis (DE) and anion and cation exchange membrane systems (AEM and CEM), were investigated for the coproduction of NaOH, HCl, H_2, and O_2 from brine solution with a concentration of 0.86 M NaCl. The influence of Pt and MnMo/Ti anode electrodes on brine

https://doi.org/10.1021/acs.energyfuels.4c00865
Energy Fuels 2024, 38, 15812–15822

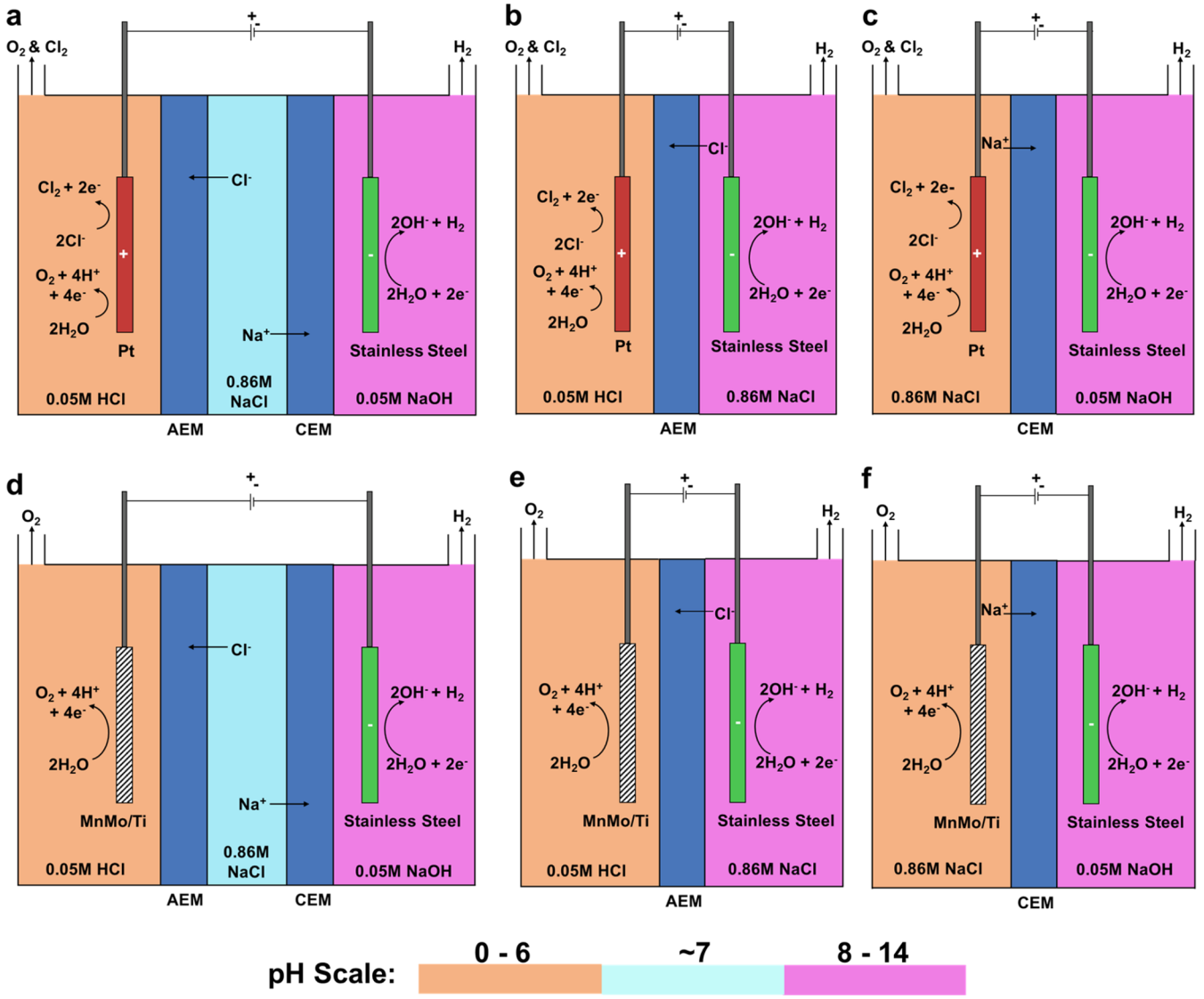

Figure 1. Schematic representation of the experimental configurations used in this study. (a) Direct electrosynthesis (DE) using the Pt anode. (b) Anion exchange membrane (AEM) electrolysis using the Pt anode. (c) Cation exchange membrane (CEM) electrolysis using the Pt anode. (d) Direct electrosynthesis (DE) using the MnMo/Ti anode. (e) Anion exchange membrane electrolysis (AEM) using the MnMo/Ti anode. (f) Cation exchange membrane electrolysis (CEM) using the MnMo/Ti anode.

electrolysis was investigated in all systems. Compared to the BMED system, which utilized multiple membranes, including one or more bipolar membranes that prevent the formation of chlorine gas in the anode, the DE system uses only cation and anion exchange membranes, resulting in a more simplified configuration that avoids the use of bipolar membrane(s) (Figure 1a).[9,18] However, DE systems usually generate Cl_2 gas along with O_2 gas at the anode (reaction R3). The corrosivity and toxicity of Cl_2 gas make it challenging to develop and scale up DE systems. Furthermore, the anode materials currently available promote chlorine gas evolution instead of oxygen gas formation, motivating the need for anodes that promote Cl_2 gas suppression. The water splitting at the anode to produce O_2 and H^+ ions is represented in reaction R1 below.[9] On applying an electric field, Cl^- ions are transported to the anode chamber and react with the generated protons to produce HCl (reaction R2). H_2 and hydroxide ions are produced at the cathode, as represented by reaction R4. As shown in reaction R5, the hydroxide ions then react with Na^+ ions to form NaOH. The overall target reaction for brine electrolysis is shown in reaction R6, while the possible undesired reaction (reaction R7) may also occur.[19]

anode: $$H_2O \rightarrow \frac{1}{2}O_{2(g)} + 2H^+ + 2e^- \quad (E^0 = 1.23\ V) \tag{R1}$$

$$2H^+ + 2Cl^- \rightarrow 2HCl_{(aq)} \tag{R2}$$

possible side reaction at anode: $$2Cl^- \rightarrow Cl_{2(g)} + 2e^- \quad (E^0 = 1.26\ V) \tag{R3}$$

cathode: $$2H_2O_{(l)} + 2e^- \rightarrow H_{2(g)} + 2OH^- \tag{R4}$$

$$2OH^- + 2Na^+ \rightarrow 2NaOH_{(aq)} \tag{R5}$$

ideal: $$2NaCl_{(2)} + 3H_2O_{(l)} \rightarrow H_{2(g)} + \frac{1}{2}O_{2(g)} + 2HCl_{2(aq)} + 2NaOH_{(aq)} \tag{R6}$$

https://doi.org/10.1021/acs.energyfuels.4c00865
Energy Fuels 2024, 38, 15812−15822

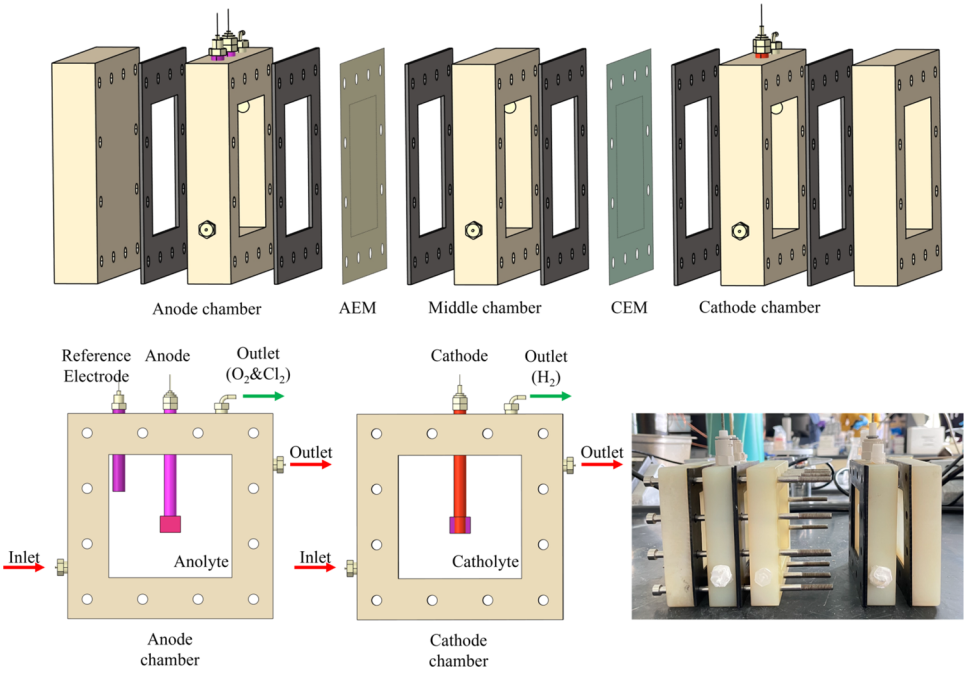

Figure 2. Assembly of the customized 3D printed cell for brine electrolysis is shown. This cell is composed of three chambers and two end plates.

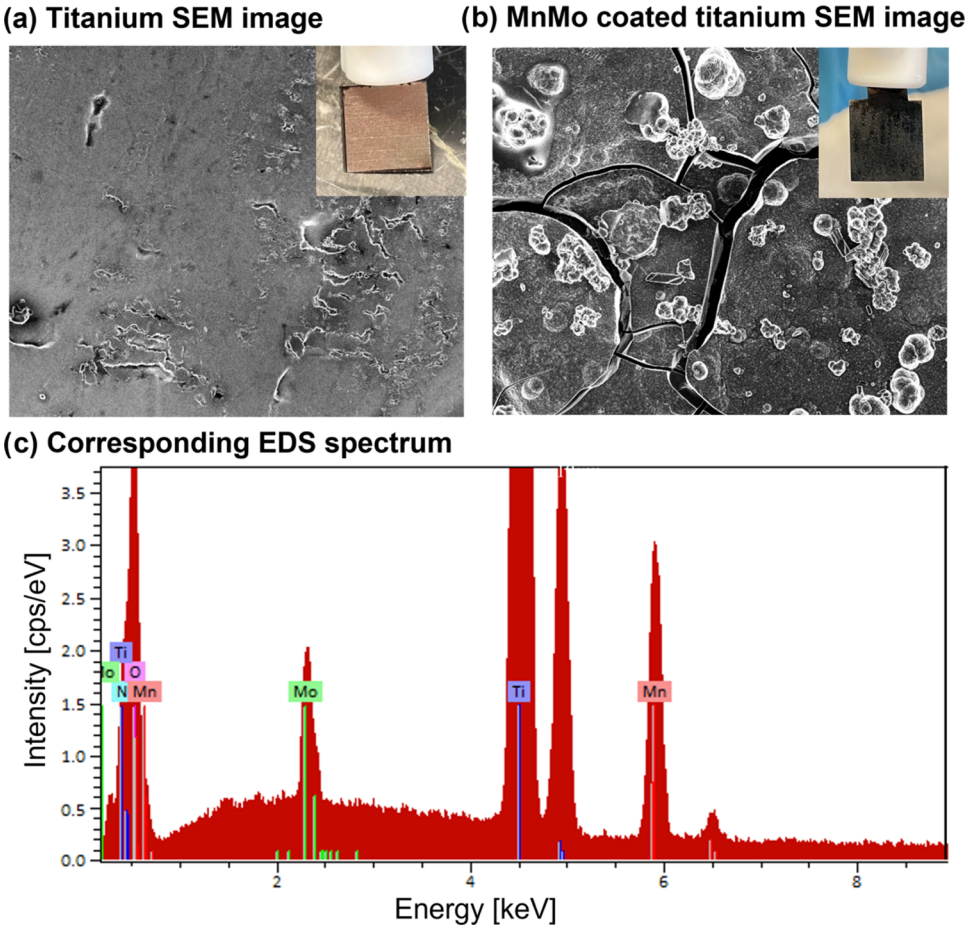

Figure 3. Morphology of the (a) titanium matrix and (b) MnMo-coated titanium material (MnMo/Ti) are represented in the SEM images. (c) The corresponding EDS spectrum of the MnMo/Ti material is shown.

https://doi.org/10.1021/acs.energyfuels.4c00865
Energy Fuels 2024, 38, 15812−15822

undesired:

$$2NaCl_{(aq)} + 2H_2O_{(l)} \rightarrow H_{2(g)} + Cl_{2(g)} + 2NaOH_{(aq)} \quad (R7)$$

As shown in Figure 1b,c, only one membrane was used in the AEM and CEM systems; however, both anion and cation exchange membranes were used in the DE system. In the AEM system, NaCl solution was placed in the cathode chamber separated from the anode chamber by using the anion exchange membrane. During electrolysis, the AEM allows for Cl^- transfer from the cathode chamber to the anode chamber to produce HCl, as shown in reactions R1 and R2. In the cathode chamber, the OH^- ions generated during water splitting are then combined with available Na^+ ions to produce NaOH, as shown in reactions R4 and R5. Similarly, the CEM system used a cation exchange membrane that allowed the transfer of Na^+ from the anode to the cathode to produce HCl and NaOH. It is important to note that both AEM and CEM systems simultaneously produced O_2 and Cl_2 at the anode.

During the experiment, a current density of 90 mA/cm^2 was applied by the galvanostat method for 5 h. The DE cell was operated in a batch mode, with an anolyte consisting of HCl solution (0.05 M, 50 mL), a catholyte consisting of NaOH solution (0.05 M, 50 mL), and the solution in the central compartment consisting of NaCl solution (0.86 M, 50 mL). The central compartment was separated from the anolyte and catholyte by the AEM and CEM, respectively. The aqueous solutions were injected into their respective chambers by using a peristaltic pump at the start of each batch experiment.

Electrochemical Cell. The design of the brine electrolysis cell is shown in Figure 2. The cell has two end plates and three compartments with outer dimensions of 10 × 10 × 2 cm^3, totaling a volume of 72 cm^3. The customized cell was built using a three-dimensional (3D) printer with a polyethylene material that can withstand both acidic and basic conditions. The anode compartment has openings for the anode, gas outlet, and reference electrode. The cathode compartment has openings for the cathode (made of stainless steel, 26 × 24 mm^2) and a gas outlet. The cell also has six gaskets made of ethylene propylene diene monomer (EPDM) rubber with a thickness of 1.6 mm, and the dimension of each gasket is 10 cm × 10 cm. Two gaskets are placed between compartments to secure ion exchange membranes and prevent the leakage of gaseous products. The size of the used anion exchange membrane (AEM, Fumasep FAM) and cation exchange membrane (CEM, Nafion 117) is 10 cm × 10 cm. The two end plates provide support to the three compartments, and 12 holes (diameter 5 mm) are made to join the five compartments. Twelve clamping bolts are also inserted. All brine electrolysis experiments were conducted with a current density of 90 mA/cm^2 for 5 h, in which a potentiostat (Interface 1010E, Gamry Instruments) was employed. For the Pt cases, the anode surface area was 2.25 cm^2, and a total charge of 3647 C was supplied for each test. In the MnMo/Ti case, the anode area was 1 cm^2, and 1621 C was supplied.

Fabrication of Manganese–Molybdenum Oxide Anode. An anodic deposition strategy is utilized to fabricate a MnMo-coated titanium anode. In detail, a mixture of 0.4 M $MnSO_4$ and 0.003 M Na_2MoO_4 is used as the electrolyte. The anode is made of titanium with dimensions of 10 × 10 × 1 mm^3, while the cathode is made of platinum with dimensions of 15 × 15 × 1 mm^3. A constant current density of 60 mA/cm^2 is applied at a temperature of 90 °C for 1 h.[20] By the use of H-type cells, a suitable separation is ensured between the anode and the cathode. When a potential is applied, manganese and molybdenum ions migrate toward the anode, enabling their deposition onto the titanium surface.

After the reaction, manganese and molybdenum are found to have been anodically deposited on the titanium surface. The morphology of the materials is studied using a scanning electron microscope, specifically using a Zeiss LEO 1550 FESEM instrument. The formation of titanium and MnMo-coated titanium is evident from the scanning electron microscopy (SEM) images (Figure 3a,b). Also, energy-dispersive X-ray spectroscopy (EDS) mappings show a strong signal of Mn and Mo in the fabricated MnMo-coated titanium anode (Figure 3c).

Product Analyses. The concentrations of HCl and NaOH are determined by titration using standard solutions of 0.5 M HCl and 0.5 M NaOH. The purity of the HCl solutions was determined by quantifying the amount of Na^+ in the solution using inductively coupled plasma-optical emission spectrometry (ICP-OES, Thermo Fisher Scientific, iCAP PRO). The volume of hydrogen produced at the cathode is measured using a gas flow meter (OMEGA FMA1808A). The gas produced in the anode is passed through a solution of KI with a concentration of 25 g/500 mL. Cl_2 can be retained in solution through reaction R8.[21] The chlorine gas undergoes a substitution reaction with the I^- ions to produce I_2. As Cl_2 reacts with the KI solution, the transparent KI solution changes to reddish brown. The concentration of I_2 is determined through iodometric titration using ascorbic acid (0.0008 M) and starch (reaction R9).[21] When the titration reaches the end point, the ascorbic acid turns from transparent to purple, indicating that the I_2 has been fully reacted. The concentration of I_2 can be calculated by using eq 1. With the concentration of I_2 known, the concentration of Cl_2 gas can also be calculated. The volume of Cl_2 can be determined by the volume of the KI solution (500 mL) used in the experiment. It is important to note that if the concentration of Cl_2 gas is below 10 ppm, then the iodometric titration method may not be reliable. In this case, the kit is used for chlorine measurement (chemworld QCTK1120-Z).

$$Cl_2 + 2I^- \rightarrow 2Cl^- + I_2 \quad (R8)$$

$$C_6H_8O_6 + I_2 \rightarrow C_6H_6O_6 + 2I^- + 2H^+ \quad (R9)$$

$$M_{\text{ascorbic acid}} \times V_{\text{ascorbic acid}} = M_{\text{Iodine}} \times V_{\text{Iodine}} \quad (1)$$

In the experiments involving the production of chlorine gas and oxygen gas through electrolysis, it is assumed that the generated electrons are utilized in the production of these gases on the anode side. The amount of Cl_2 gas produced can be determined through iodometric titration, which also enables calculation of the number of electrons utilized in its production. The amount of O_2 gas produced can then be calculated by subtracting the total number of electrons used for Cl_2 production from the total number of electrons generated (eq 2).

$$O_{2\ \text{produced}}\ (\text{mol}) = \frac{\text{total e}^-\ (\text{mol}) - \text{e}^-\ \text{used in Cl}_2\ (\text{mol})}{4} \quad (2)$$

Revenue Calculations. In this study, revenues were computed by assuming that a 1 MW electrolyzer unit was set up. The estimated revenues for various routes to produce H_2 and associated products such as HCl and NaOH for a year can be determined using eq 3. More information on these calculations can be found in the Supporting information.

$$\frac{\text{estimated revenue}}{\text{year}} = \frac{\text{H}_2\ \text{revenue} + \text{NaOH revenue} + \text{HCl revenue}}{\text{year}} \quad (3)$$

RESULTS AND DISCUSSION

To address the key knowledge gaps associated with the direct electrosynthesis of brine, including the extent of Cl_2 gas suppression achieved using MnMo on Ti electrodes, the quantity of coproduct generation associated with Cl_2 gas suppression, and the associated economics, detailed experimental studies were conducted. The effectiveness of MnMo on Ti electrodes on the suppression of Cl_2 gas evolution is evaluated and compared to a base case, which involves the use of Pt electrodes. These results are discussed in detail below.

Chlorine Evolution Reaction (CER). Chlorine evolution reaction (CER) is likely to co-occur with oxygen evolution reaction (OER) during brine electrolysis (reactions R1 and R3). Although CER theoretically requires a higher potential than

https://doi.org/10.1021/acs.energyfuels.4c00865
Energy Fuels 2024, 38, 15812−15822

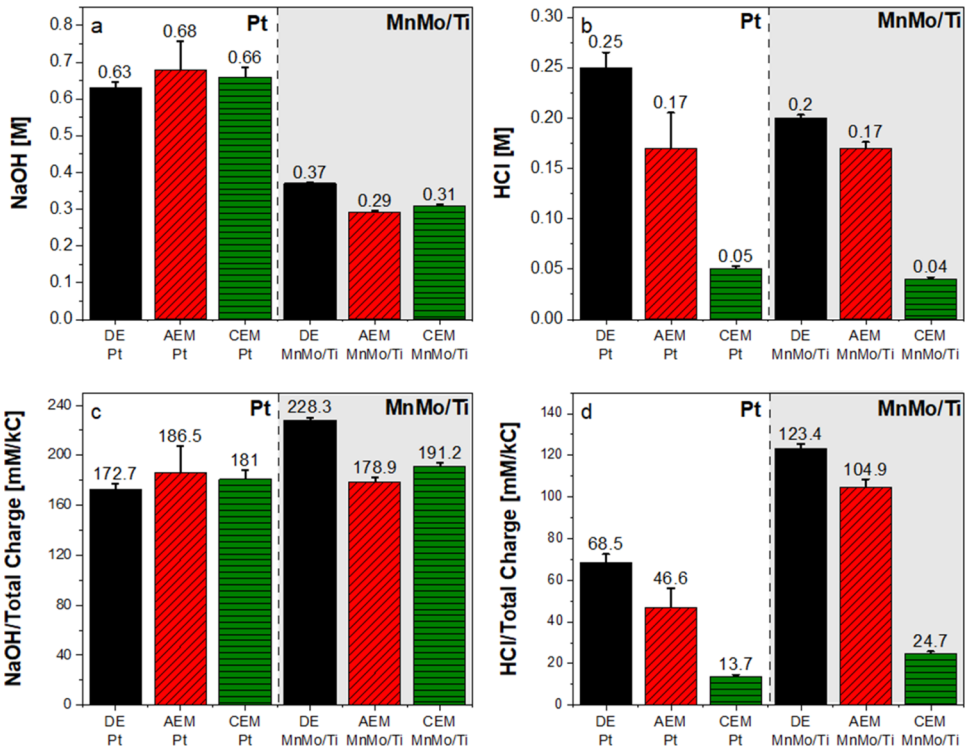

Figure 4. Comparison of HCl and NaOH concentrations when Pt and MnMo/Ti anodes are used in various electrolysis systems, including direct electrosynthesis (DE), anion exchange membrane electrolysis (AEM), and cation exchange membrane electrolysis (CEM) systems, is shown. (a) The absolute concentration of NaOH produced. (b) The absolute concentration of HCl produced. (c) Charge normalized concentration of NaOH produced. (d) Charge normalized concentration of HCl produced.

OER from a thermodynamic perspective, CER is kinetically more favorable than OER majorly because CER requires two electrons per mol of Cl_2, while O_2 requires four electrons.[22] In this context, the selectivity of the anode material becomes essential in direct electrosynthesis to inhibit the production of Cl_2. Manganese (Mn)- and molybdenum (Mo)-doped materials have been reported for water electrolysis using saline water.[23,24] For instance, a manganese−molybdenum−tungsten oxide-deposited IrO_2-coated titanium substrate anode was reported to suppress Cl_2 formation and favor OER.[20] More recently, thin films of MnO_x have been electrodeposited onto glassy carbon-supported hydrous IrO_x, which can significantly reduce the CER, thereby making it a highly OER-selective catalyst.[25] A Cl^- blocking layer mechanism is proposed to explain their high OER selectivity, demonstrating that MnO_x overlayers can effectively block the diffusion of Cl^- ions, resulting in CER suppression.[24] While these studies have shown the efficacy of manganese (Mn)- and molybdenum (Mo)-doped materials in enhancing the OER over CER, the effect of Cl_2 suppression on the production of HCl or NaOH has not been reported. In this study, a MnMo-coated titanium anode is elaborately fabricated via electrodeposition, noted as MnMo/Ti. Furthermore, a series of experiments are conducted to evaluate its performance on DE, AEM, and CEM systems for the coproduction of H_2, O_2, HCl, and NaOH.

NaOH and HCl Production under Different Scenarios. The yields of NaOH and HCl are examined in various electrode and membrane configurations. Normalization of the data is essential due to the variation in the total charge supplied to the platinum (Pt) and MnMo/Ti electrodes. A higher total charge supplied of 3647 C was observed using a Pt anode compared to 1621 C when the MnMo/Ti anode was used after 5 h of operation. The difference in charge supply between the MnMo/Ti electrode (2.25 cm^2) and Pt electrode (1 cm^2) is attributed to their different surface areas (see the Materials and Methods section for more details). Consequently, it becomes apparent that the Pt cases should exhibit a higher production of NaOH compared to the scenario, where MnMo/Ti electrodes are used (Figure 4a). Without normalization to the total charge, NaOH yields are suppressed by 41.3, 57.4, and 53.0% for DE, AEM, and CEM, respectively, using the MnMo/Ti anode compared to the use of Pt electrodes. To ensure data comparability, normalization of the NaOH concentrations to the total charge is necessary. On normalizing the NaOH concentrations with the total charge, compared values are obtained using Pt and MnMo/Ti anodes in the range of 172.7−228.3 mM/kC (Figure 4c). It is also interesting to note that DE with the MnMo/Ti anode results in the highest normalized yield of 228.3 mM/kC.

In contrast, the lower absolute and normalized yields of HCl compared to NaOH are nontrivial. As shown in reactions R6 and R7, either OER or CER pathway should not affect the concentration of NaOH theoretically; however, the concentration of HCl is strongly dependent on Cl_2 suppression. As shown in Figure 4b, the concentrations of produced HCl are in the range of 0.04−0.25 M, which is significantly lower than the range of 0.31−0.63 M NaOH. Furthermore, the lower HCl concentration could also be due to the phenomenon of back diffusion when the protons produced in the anode chamber migrate to the middle chamber. This phenomenon occurs when there is a gradient of proton concentration across the anion exchange membrane, causing some protons to be transported back across the membrane to the side with lower proton concentrations.[26] Without normalization, MnMo/Ti and Pt anodes resulted in HCl concentrations of 0.25 and 0.20 M,

https://doi.org/10.1021/acs.energyfuels.4c00865
Energy Fuels 2024, 38, 15812−15822

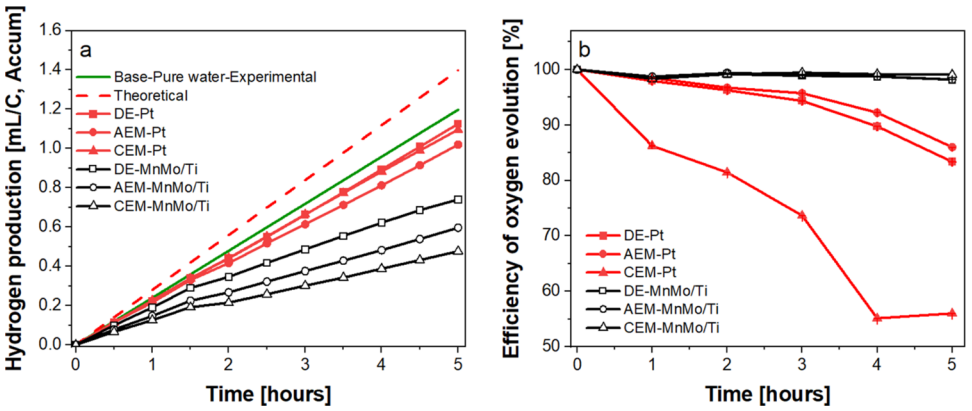

Figure 5. Charge normalized H_2 volumes produced using the Pt and MnMo/Ti anodes compared to base case−pure water Pt systems and theoretical volumes and (b) efficiencies of oxygen evolution at the Pt and MnMo/Ti anodes for direct electrosynthesis (DE), anion exchange membrane electrolysis (AEM), and cation exchange membrane electrolysis (CEM) systems are shown. Results for H_2 and O_2 gas evolution are summarized in Tables S1−S3.

respectively, in a DE setup. In contrast, HCl concentrations obtained using AEM and CEM with Pt and MnMo/Ti anodes are lower, with CEM resulting in the lowest concentrations of HCl. After normalization, HCl concentrations are 123.4 and 68.5 mM/kC for DE with MnMo/Ti and Pt anodes, respectively. The use of MnMo/Ti anodes in all configurations, including DE, CEM, and AEM, results in higher normalized HCl concentrations compared to when Pt anodes are used (Figure 4d). It is interesting to note that the CEM system produced the lowest amount of HCl, regardless of the type of anode used. This phenomenon can be explained by the fact that the CEM anolyte is composed of NaCl at a concentration of 0.86 M, which results in a higher initial concentration of Cl^- ions when compared to the DE and AEM systems, in which the concentration of Cl^- ions is 0.05 M. As a result, a significant amount of chlorine gas is generated, which in turn reduces the amount of HCl produced. Also, the phenomenon of back diffusion is more pronounced in CEM setup compared to DE or AEM setup (Figure 4b,d). The purity of HCl obtained from DE and AEM is determined by ICP. It was observed that the final HCl solutions contained 2.29% (±0.05) and 7.37% (±0.38) of Na^+ impurities for DE and AEM setups, respectively. To obtain a higher purity HCl product, the quality and selection of the membrane are of great importance and should be carefully considered.

The relatively lower concentrations of NaOH (0.31−0.63 M) and HCl (0.04−0.25 M) produced, compared to some reported works, can be attributed to the lower current densities used and fixed concentration of artificial brine supply. Higher concentrations of NaOH and HCl can be obtained by utilizing refreshed brine with a continuous flow, thereby ensuring more availability of Na and Cl ions for base and acid production. Moreover, obtaining a more concentrated NaOH and HCl production would require higher current densities and longer operating time.[27,28]

H_2 Evolution in DE, CEM, and AEM Systems. To investigate the influence of MnMo/Ti and Pt anodes in DE, CEM, and AEM configurations on H_2 evolution, brine electrolysis experiments are conducted at a current density of 90 mA/cm^2 for 5 h. The theoretical amount of H_2 produced was calculated using stoichiometric values obtained from reaction R4 to be 0.46 L for Pt and 0.21 L for MnMo/Ti after 5 h of constant current supply. To establish a practical baseline for comparison, an electrolysis experiment with pure water was conducted without membranes using 0.2 M H_2SO_4 and a volume of 150 mL. At the end of the electrolysis, 0.4 L of H_2 was obtained, which was lower than the theoretical amount calculated (0.46 L) based on the total charge supplied. The lower H_2 produced was attributed to factors, such as flow meter error, and subsequent H_2 efficiencies for brine electrolysis were computed relative to the baseline experiments.

Additionally, normalizing the absolute H_2 volume produced to the total charge is essential for an accurate comparison. The theoretical normalized H_2 volumes for both the Pt and MnMo/Ti electrodes are similar as shown in Figure 5a. The calculated efficiencies of H_2 production at the Pt anode range from 79 to 81% with the normalized value. The highest levels of H_2 evolution are obtained from the DE system at the Pt anode (81%), followed by CEM and AEM systems. In contrast, the H_2 evolution efficiencies of the MnMo/Ti anode are found to be in the range of 35−54% with the normalized value, which is much lower than those of the Pt anode. Compared to systems using CEM and AEM systems, DE systems exhibited the best performance (54%) using the MnMo/Ti anode. The H_2 production rates are also calculated for further comparison. For the Pt electrode, the measured H_2 production rates range from 0.204 to 0.226 mL/h·C, while they range from 0.095 to 0.148 mL/h·C for the MnMo/Ti electrode. One of the approaches to increase the performance of MnMo/Ti anodes is to explore the use of other metals as dopants and enhance their stability and performance in acidic environments.

O_2 Evolution Efficiency in DE, CEM, and AEM Systems. In these experiments, Cl_2 and O_2 gases are produced at the anode during electrolysis. It is assumed that all of the generated electrons are utilized in the production of these gases. The oxygen evolution efficiency is examined to evaluate the effectiveness of Cl_2 suppression, as it competes with the CER. As shown in Figure 5b, the highest oxygen evolution efficiency of 98.1% is observed in the presence of MnMo/Ti anodes in CEM systems, while the DE and AEM systems with the same anode show comparable results around 96%. In contrast, O_2 evolution efficiency is 86, 84, and 56% in AEM, DE, and CEM systems with Pt anodes after 5 h of operation (Figure 5b). In other words, the CEM system with the Pt anode resulted in the highest proportion of Cl_2 gas evolution, which is also in agreement with the lower HCl concentration obtained with the CEM system. Therefore, these results conclusively demonstrate that the MnMo/Ti anode can effectively suppress CER.

https://doi.org/10.1021/acs.energyfuels.4c00865
Energy Fuels 2024, 38, 15812−15822

Table 2. Energy Consumption for Brine Electrolysis Using Pt and MnMo/Ti Electrodes in Various Configurations, Including Direct Electrosynthesis (DE), Cation Exchange Membrane (CEM), and Anion Exchange Membrane (AEM)[a]

				HCl concentration		NaOH concentration				
anode	system	average potential (V)	current density (mA/cm^2)	initial (M)	final (M)	initial (M)	final (M)	system energy consumption (Wh)	normalized energy consumption (kWh/kg_{HCl})	normalized energy consumption (kWh/kg_{NaOH})
Pt	base	2.6	90					2.6		
Pt	DE	2.7	90	0.05	0.3	0.05	0.68	2.8	6.1	2.2
Pt	AEM	2.8	90	0.05	0.22		0.68	2.8	9.2	2.1
Pt	CEM	3.2	90		0.05	0.05	0.71	3.2	35.5	2.4
MnMo/Ti	DE	5.9	90	0.05	0.25	0.05	0.42	2.7	7.3	3.6
MnMo/Ti	AEM	7.0	90	0.05	0.22		0.29	3.1	10.1	5.3
MnMo/Ti	CEM	5.8	90		0.04	0.05	0.36	2.6	35.9	4.2

[a]Concentration values are approximated to two decimal places, whereas other reported values are approximated to one decimal place.

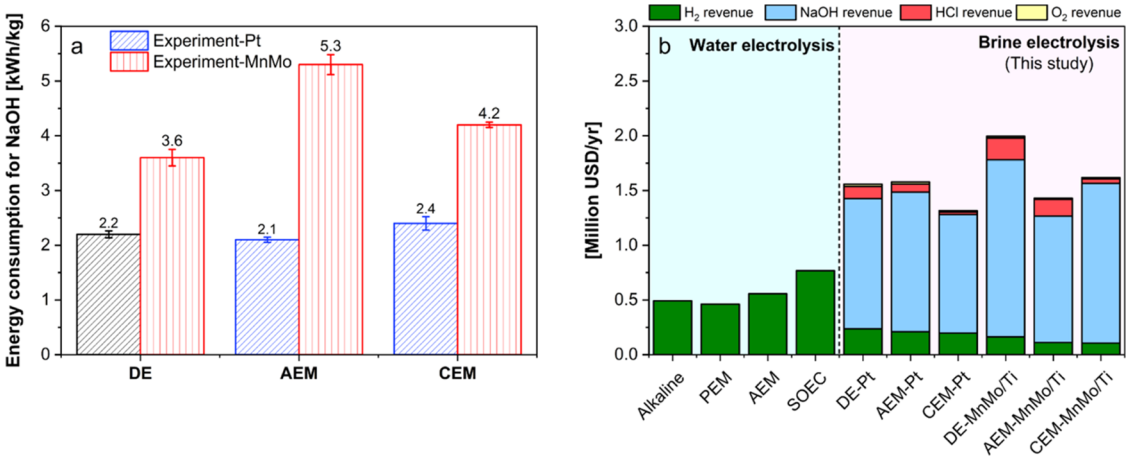

Figure 6. (a) Comparison of the energy consumption for NaOH production using direct electrosynthesis (DE), anion exchange membrane electrolysis (AEM), and cation exchange membrane electrolysis (CEM) systems based on experimental studies is shown. The influence of using Pt compared to the MnMo/Ti electrode on the energy consumption is also reported. (b) Estimated revenues for using electrolysis routes assuming the use of a 1 MW electrolyzer are shown. Current efficiencies underlying these estimates are reported in Table S4. The details and assumptions resulting in these estimates are noted in Tables S5−S7 in the Supporting Information (SI).

Analyses of Energy Consumption. One of the key considerations associated with the scalability of brine electrolysis pathways is the overall energy consumption in DE, CEM, and AEM systems using Pt or MnMo/Ti anodes. To this end, the associated energy consumptions are determined for these systems of interest. As shown in Table 2, the DE system has the lowest energy consumption (2.7 Wh) when using a Pt electrode. However, the energy consumption associated with AEM and CEM systems is higher at 2.8 and 3.2 Wh, respectively, indicating that using fewer membranes does not necessarily result in lower energy consumption compared to DE. When MnMo/Ti electrodes are used, a higher potential is required to achieve the same current density, resulting in a higher energy consumption. The result shows that the MnMo/Ti electrode consumes more energy than the Pt electrode, which could be caused by its relatively smaller exposed surface area and its lower electrode activity.

To facilitate a comprehensive comparison among the different experimental conditions, the energy consumption values were normalized with respect to the produced NaOH, HCl, and H_2. This normalization approach ensures a fair assessment of energy efficiency (see the Supporting Information for more details). Energy consumption normalized by NaOH is the most common indicator for evaluation. The results indicate that the utilization of MnMo/Ti electrodes led to higher energy consumption (3.6−5.3 kWh/kg_{NaOH}) compared to Pt electrodes (2.1−2.4 kWh/kg_{NaOH}) as shown in Figure 6a. The lower energy consumption observed with the Pt electrode is due to the lower overpotential required for water-salt splitting. Nonetheless, the DE system shows promise in saving energy. An energy consumption of 2.2 kWh/kg_{NaOH} was observed with Pt in the DE system, which is lower than the reported energy consumption of BMED systems, consuming 3.6 kWh/kg_{NaOH}.[29] Similar results can also be observed when comparing the energy consumption of HCl and H_2 (Table 2), where Pt electrodes demonstrate greater energy efficiency. These performances of Pt are competitive with those reported in recent studies of BMED systems. However, the relatively higher energy consumption of HCl (6.1−35.9 kWh/kg_{HCl}) compared to reported studies may be attributed to the back diffusion of protons, resulting in lower yields of HCl.[18,30] With the MnMo/Ti anode, the DE system demonstrates the lowest normalized energy consumption of 3.6 kWh/kg_{NaOH} compared to the CEM (4.2 kWh/kg_{NaOH}) and AEM (5.3 kWh/kg_{NaOH}) systems. These results highlight the importance of developing novel anode materials with energy consumption considerations for application in a DE system. Anode materials should also be elaborately constructed to favor OER reactions over CER reactions to achieve this goal.[31]

Moreover, the energy consumption of AEM and CEM was as high as that of the DE system, even though they used fewer

https://doi.org/10.1021/acs.energyfuels.4c00865
Energy Fuels 2024, 38, 15812−15822

membranes than DE or BMED. This observation is explained by the fact that AEM and CEM use NaCl solution as the catholyte and anolyte, respectively. Since the initial pH of a NaCl solution is between 6 and 7.3, the basicity and acidity increase more rapidly in AEM and CEM systems as the reaction progresses. These changes in pH lead to higher energy consumption. During brine electrolysis, the HER and the OER are the main reactions, and their rates and thermodynamic potentials are pH-dependent. The HER reaction is favored at low pH, while the OER reaction is favored at high pH.[32] If the pH of the electrolyte changes significantly during the electrolysis process, the relative rates of the HER and OER reactions can shift, leading to an imbalance in the production of H_2 and O_2 gases. This change can result in lower Faradaic efficiency and higher energy consumption.

Estimated Revenue Potential. Successful scalability of the proposed brine electrolysis routes using DE, AEM, and CEM systems is dependent on the overall economic feasibility. Conventional H_2 production method via steam methane reforming (SMR) using natural gas costs U.S. $1.3/kg.[33] However, green H_2 production using freshwater electrolyzers (e.g., alkaline electrolyzer) has been estimated to cost around U.S. $2/kg or higher.[34] In the case of brine electrolysis, the cost per kilogram of H_2 could be higher due to comparably lower H_2 yields as a result of competing reactions, such as in reaction R3. Nonetheless, the decreasing cost of renewable energy has continued to motivate electrochemically driven processes for chemical transformations.[35,36] In particular, chemical transformations that facilitate the coproduction of multiple high-valued products in fewer steps are of great interest.[27]

One of the most promising aspects of brine electrolysis is that it also produces valuable byproducts, such as NaOH and HCl. These byproducts offset the costs associated with H_2 production. As shown in Figure 6b, the estimated revenue potential can be significantly improved through the sale of byproducts, such as O_2, NaOH, and HCl. This improvement is primarily caused by the coproduction of NaOH, which accounts for 87−97% of the additional revenue generated. In fact, even in the MnMo/Ti case, which has high energy consumption, the overall economic feasibility could be better than that of alkaline and proton exchange membrane (PEM) electrolyzers for green H_2 production. Using DE systems with MnMo/Ti electrodes, the revenue generated per year was estimated to be 4 times higher than that of alkaline electrolysis using pure water. This change can be attributed to the coproduction of value-added products, such as NaOH and HCl. The primary basis for calculating the expected revenue is shown in Table S6. While the cost of conventional electrolyzers using pure water has been widely investigated, information about brine electrolysis is limited due to its lack of commercialization. Furthermore, the selling prices of H_2, NaOH, and HCl are assumed to be based on U.S. prices.[37] It is important to note that these analyses were conducted by assuming a synthetic brine feedstock comprised of NaCl solution; most brine solutions are not purely NaCl so the purity of final NaOH and HCl produced should be a consideration in real systems.

CONCLUSIONS

This study demonstrates the scientific and economic feasibility of coproducing multiple high-value products, such as H_2, O_2, NaOH, and HCl, via brine electrolysis using various configurations, including direct electrosynthesis (DE) without bipolar membranes, cation exchange membranes (CEMs), and anion exchange membranes (AEMs) using Pt and MnMo/Ti electrodes. The challenge of suppressing Cl_2 evolution with Pt electrodes was effectively addressed through the development of the MnMo/Ti electrode, which demonstrated a superior performance in suppressing Cl_2 evolution at the anode, making it a promising alternative to Pt electrodes. The experimental findings revealed that direct electrosynthesis using the MnMo/Ti electrode resulted in the highest production of NaOH and HCl when the results were normalized to the charge supply. Our studies revealed that a key future direction lies in achieving multiple cycles of performance for suppressing Cl_2 evolution using other stable electrodes, which could further reduce the energy consumption.

With respect to H_2 production, Pt electrode systems (DE, CEM, and AEM) were found to exhibit better economic performance compared with scenarios involving the use of MnMo/Ti electrodes. However, the overall economic performance of MnMo/Ti electrodes can be significantly improved considering the coproduction of O_2, NaOH, and HCl. In conclusion, the findings of this study demonstrate the potential of brine electrolysis as a sustainable and cost-effective approach for H_2 production in addition to the corecovery of multiple products (e.g., O_2, NaOH, and HCl). This study provides an integrated approach to connect experimental studies with economic assessments to evaluate the scalable deployment of brine electrolysis systems with an inherent suppression of Cl_2 gas evolution.

ASSOCIATED CONTENT

Supporting Information

The Supporting Information is available free of charge at https://pubs.acs.org/doi/10.1021/acs.energyfuels.4c00865.

Additional experimental details, materials, and methods, including photographs of experimental setup and detailed calculations for the product(s) quantification, energy efficiencies, and economics (PDF)

AUTHOR INFORMATION

Corresponding Author

Greeshma Gadikota − *School of Civil and Environmental Engineering, Cornell University, Ithaca, New York 14853, United States; Smith School of Chemical and Biomolecular Engineering, Cornell University, Ithaca, New York 14853, United States;* orcid.org/0000-0002-6527-8316; Phone: +1 857-253-8724; Email: gg464@cornell.edu

Authors

Minkyeong Kim − *School of Civil and Environmental Engineering, Cornell University, Ithaca, New York 14853, United States*

Peilong Lu − *School of Civil and Environmental Engineering, Cornell University, Ithaca, New York 14853, United States*

Prince Ochonma − *Smith School of Chemical and Biomolecular Engineering, Cornell University, Ithaca, New York 14853, United States;* orcid.org/0000-0003-0297-0919

Complete contact information is available at: https://pubs.acs.org/10.1021/acs.energyfuels.4c00865

Author Contributions

M.K.: conceptualization, methodology, visualization, validation, formal analysis, investigation, data curation, writing—original

https://doi.org/10.1021/acs.energyfuels.4c00865
Energy Fuels 2024, 38, 15812−15822

draft, visualization. P.L.: methodology, validation, formal analysis, investigation, data curation, writing—review and editing; P.O.: visualization, validation, formal analysis, data curation, writing—review and editing; G.G.: conceptualization, methodology, formal analysis, supervision, funding acquisition, project administration, writing—review and editing.

Notes

The authors declare the following competing financial interest(s): Greeshma Gadikota is the co-founder of Carbon To Stone which is advancing technologies for sustainable resource recovery and carbon management.

■ ACKNOWLEDGMENTS

The authors acknowledge the use of the shared facilities at the Cornell Center for Materials Research (CCMR), which is supported through the NSF MRSEC program (DMR-1719875). M.K. and P.L. gratefully acknowledge the support of Korea Gas Corporation and Fellowship from the School of Civil and Environmental Engineering at Cornell University, respectively. P.O.'s efforts are supported by the Link Foundation Energy Fellowship and DOE through the INSIGHT project: DE-EE0009391. G.G. is grateful for the support of DOE—Office of Fossil Energy and Carbon Management (DE-FE0032398). The authors would like to thank Paul Charles, the Technical Services Support Supervisor for the School of Civil and Environmental Engineering, Cornell University, for providing support with the fabrication of the electrolysis cell. The authors would also like to thank Akanksh Mamidala and Prarabdh Jain for providing support with ICP measurements.

■ ABBREVIATIONS

BMED, bipolar membrane electrodialysis; DE, direct electrosynthesis; AEM, anion exchange membrane; CEM, cation exchange membrane; MnMo, manganese−molybdenum; PEM, proton exchange membrane electrolyzer; SOEC, solid oxide electrolyzer cell

■ REFERENCES

(1) Bhat, S. A.; Sadhukhan, J. Process intensification aspects for steam methane reforming: An overview. *AIChE J.* **2009**, *55*, 408−422.
(2) Gadikota, G. Carbon Mineralization Pathways for Carbon Capture, Storage and Utilization. *Commun. Chem.* **2021**, *4*, No. 23.
(3) Ochonma, P.; Noe, C.; Mohammed, S.; Mamidala, A.; Gadikota, G. Integrated Low Carbon H2 Conversion with in situ Carbon Mineralization from Aqueous Biomass Oxygenate Precursors by Tuning Reactive Multiphase Chemical Interactions. *React. Chem. Eng.* **2023**, *8*, 1943−1959.
(4) Ochonma, P.; Blaudeau, C.; Krasnoff, R.; Gadikota, G. Exploring the Thermodynamic Limits of Enhanced H2 Recovery With Inherent Carbon Removal From Low Value Aqueous Biomass Oxygenate Precursors. *Front. Energy Res.* **2021**, *9*, No. 742323.
(5) Gadikota, G. Multiphase Carbon Mineralization for the Reactive Separation of CO2 and Directed Synthesis of H2. *Nat. Rev. Chem.* **2020**, *4*, 78−89.
(6) Hausmann, J. N.; Schlögl, R.; Menezes, P. W.; Driess, M. Is direct seawater splitting economically meaningful? *Energy Environ. Sci.* **2021**, *14*, 3679−3685.
(7) Janssen, C. H. C. Heavy Metal Extractions from NaCl Brines to Pseudoprotic Ionic Liquids. *Ind. Eng. Chem. Res.* **2021**, *60*, 1808−1816.
(8) Dastgheib, S. A.; Salih, H. H. Treatment of Highly Saline Brines by Supercritical Precipitation Followed by Supercritical Membrane Separation. *Ind. Eng. Chem. Res.* **2019**, *58*, 3370−3376.
(9) Kumar, A.; Phillips, K. R.; Thiel, G. P.; Schröder, U.; Lienhard, J. H. Direct Electrosynthesis of Sodium Hydroxide and Hydrochloric Acid from Brine Streams. *Nat. Catal.* **2019**, *2*, 106−113.
(10) Du, C.; Du, J. R.; Zhao, X.; Cheng, F.; Ali, M. E. A.; Feng, X. Treatment of Brackish Water RO Brine via Bipolar Membrane Electrodialysis. *Ind. Eng. Chem. Res.* **2021**, *60*, 3115−3129.
(11) Herrero-Gonzalez, M.; Ibañez, R. Technical and Environmental Feasibilities of the Commercial Production of NaOH from Brine by Means of an Integrated EDBM and Evaporation Process. *Membranes* **2022**, *12*, No. 885.
(12) Liu, Y.; Sun, Y.; Peng, Z. Evaluation of Bipolar Membrane Electrodialysis for Desalination of Simulated Salicylic Acid Wastewater. *Desalination* **2022**, *537*, No. 115866.
(13) Chen, X.; Jiang, C.; Zhang, Y.; Wang, Y.; Xu, T. Storable hydrogen production by Reverse Electro-Electrodialysis (REED). *J. Membr. Sci.* **2017**, *544*, 397−405.
(14) Pellegrino, A.; Campisi, G.; Proietto, F.; Tamburini, A.; Cipollina, A.; Galia, A.; Micale, G.; Scialdone, O. Green hydrogen production via reverse electrodialysis and assisted reverse electrodialysis electrolyser: Experimental analysis and preliminary economic assessment. *Int. J. Hydrogen Energy* **2024**, *76*, 1−15, DOI: 10.1016/j.ijhydene.2023.12.273.
(15) Blommaert, M. A.; Aili, D.; Tufa, R. A.; Li, Q.; Smith, W. A.; Vermaas, D. A. Insights and Challenges for Applying Bipolar Membranes in Advanced Electrochemical Energy Systems. *ACS Energy Lett.* **2021**, *6*, 2539−2548.
(16) Lin, H.-W.; Cejudo-Marín, R.; Jeremiasse, A. W.; Rabaey, K.; Yuan, Z.; Pikaar, I. Direct Anodic Hydrochloric Acid and Cathodic Caustic Production during Water Electrolysis. *Sci. Rep.* **2016**, *6*, No. 20494.
(17) Badjatya, P.; Akca, A. H.; Fraga Alvarez, D. V.; Chang, B.; Ma, S.; Pang, X.; Wang, E.; van Hinsberg, Q.; Esposito, D. V.; Kawashima, S. Carbon-Negative Cement Manufacturing from Seawater-Derived Magnesium Feedstocks. *Proc. Natl. Acad. Sci. U.S.A.* **2022**, *119*, No. e2114680119.
(18) Filingeri, A.; Herrero-Gonzalez, M.; O'Sullivan, J.; Rodriguez, J. L.; Culcasi, A.; Tamburini, A.; Cipollina, A.; Ibañez, R.; Ferrari, M. C.; Cortina, J. L.; Micale, G. Acid/Base Production via Bipolar Membrane Electrodialysis: Brine Feed Streams to Reduce Fresh Water Consumption. *Ind. Eng. Chem. Res.* **2024**, *63*, 3198−3210.
(19) Dionigi, F.; Reier, T.; Pawolek, Z.; Gliech, M.; Strasser, P. Design Criteria, Operating Conditions, and Nickel−Iron Hydroxide Catalyst Materials for Selective Seawater Electrolysis. *ChemSusChem* **2016**, *9*, 962−972.
(20) Matsui, T.; Habazaki, H.; Kawashima, A.; Asami, K.; Kumagai, N.; Hashimoto, K. Anodically Deposited Manganese−Molybdenum−Tungsten Oxide Anodes for Oxygen Evolution in Seawater Electrolysis. *J. Appl. Electrochem.* **2002**, *32*, 993−1000.
(21) Abdel-Aal, H. K.; Sultan, S. M.; Hussein, I. A. Parametric Study for Saline Water Electrolysis: Part II—Chlorine Evolution, Selectivity and Determination. *Int. J. Hydrogen Energy* **1993**, *18*, 545−551.
(22) Maril, M.; Delplancke, J.-L.; Cisternas, N.; Tobosque, P.; Maril, Y.; Carrasco, C. Critical Aspects in the Development of Anodes for Use in Seawater Electrolysis. *Int. J. Hydrogen Energy* **2022**, *47*, 3532−3549.
(23) Lu, X.; Pan, J.; Lovell, E.; Tan, T. H.; Ng, Y. H.; Amal, R. A Sea-Change: Manganese Doped Nickel/Nickel Oxide Electrocatalysts for Hydrogen Generation from Seawater. *Energy Environ. Sci.* **2018**, *11*, 1898−1910.
(24) Tong, W.; Forster, M.; Dionigi, F.; Dresp, S.; Sadeghi Erami, R.; Strasser, P.; Cowan, A. J.; Farràs, P. Electrolysis of Low-Grade and Saline Surface Water. *Nat. Energy* **2020**, *5*, 367−377.
(25) Vos, J. G.; Wezendonk, T. A.; Jeremiasse, A. W.; Koper, M. T. M. MnOx/IrOx as Selective Oxygen Evolution Electrocatalyst in Acidic Chloride Solution. *J. Am. Chem. Soc.* **2018**, *140*, 10270−10281.
(26) Vallejo, M. E.; Persin, F.; Innocent, C.; Sistat, P.; Pourcelly, G. Electrotransport of Cr(VI) through an Anion Exchange Membrane. *Sep. Purif. Technol.* **2000**, *21*, 61−69.
(27) Herrero-Gonzalez, M.; Diaz-Guridi, P.; Dominguez-Ramos, A.; Irabien, A.; Ibañez, R. Highly Concentrated HCl and NaOH from Brines Using Electrodialysis with Bipolar Membranes. *Sep. Purif. Technol.* **2020**, *242*, No. 116785.

(28) Herrero-Gonzalez, M.; Diaz-Guridi, P.; Dominguez-Ramos, A.; Ibañez, R.; Irabien, A. Photovoltaic Solar Electrodialysis with Bipolar Membranes. *Desalination* **2018**, *433*, 155−163.
(29) Reig, M.; Casas, S.; Valderrama, C.; Gibert, O.; Cortina, J. L. Integration of Monopolar and Bipolar Electrodialysis for Valorization of Seawater Reverse Osmosis Desalination Brines: Production of Strong Acid and Base. *Desalination* **2016**, *398*, 87−97.
(30) Yang, Y.; Gao, X.; Fan, A.; Fu, L.; Gao, C. An Innovative Beneficial Reuse of Seawater Concentrate Using Bipolar Membrane Electrodialysis. *J. Membr. Sci.* **2014**, *449*, 119−126.
(31) Kumar, A.; Du, F.; Lienhard, J. H. V. Caustic Soda Production, Energy Efficiency, and Electrolyzers. *ACS Energy Lett.* **2021**, *6*, 3563−3566.
(32) Zhu, W.; Fu, X.; Wang, A.; Ren, M.; Wei, Z.; Tang, C.; Sun, X.; Wang, J. Energy-Efficient Electrolytic H_2 Production and High-Value Added H_2-Acid-Base Co-electrosynthesis Modes Enabled by a Ni_2P Catalyst in a Diaphragm Cell. *Appl. Catal., B* **2022**, *317*, No. 121726.
(33) Katebah, M.; Al-Rawashdeh, M.; Linke, P. Analysis of Hydrogen Production Costs in Steam-Methane Reforming Considering Integration with Electrolysis and CO_2 Capture. *Cleaner Eng. Technol.* **2022**, *10*, No. 100552.
(34) Udrea, I.; Capat, C.; Olaru, E. A.; Isopescu, R.; Mihai, M.; Mateescu, C. D.; Bradu, C. Vaterite Synthesis via Gas−Liquid Route under Controlled pH Conditions. *Ind. Eng. Chem. Res.* **2012**, *51*, 8185−8193.
(35) Ochonma, P.; Gao, X.; Gadikota, G. Tuning Reactive Crystallization Pathways for Integrated CO_2 Capture, Conversion, and Storage via Mineralization. *Acc. Chem. Res.* **2024**, *57*, 267−274.
(36) Fu, X.; Pedersen, J. B.; Zhou, Y.; Saccoccio, M.; Li, S.; Sažinas, R.; Li, K.; Andersen, S. Z.; Xu, A.; Deissler, N. H.; Mygind, J. B. V.; Wei, C.; Kibsgaard, J.; Vesborg, P. C. K.; Nørskov, J. K.; Chorkendorff, I. Continuous-flow Electrosynthesis of Ammonia by Nitrogen Reduction and Hydrogen Oxidation. *Science* **2023**, *379*, 707−712.
(37) Ohgushi, H.; Okumura, M.; Yoshikawa, T.; Inboue, K.; Senpuku, N.; Tamai, S.; Shors, E. C. Bone Formation Processin Porous Calcium Carbonate and Hydroxyapatite. *J. Biomed. Mater. Res.* **1992**, *26*, 885−895.
(38) Hussain, A.; Yan, H.; Ul Afsar, N.; Jiang, C.; Wang, Y.; Xu, T. Multistage-Batch Bipolar Membrane Electrodialysis for Base Production from High-Salinity Wastewater. *Front. Chem. Sci. Eng.* **2022**, *16*, 764−773.
(39) Chen, Q.-B.; Wang, J.; Liu, Y.; Zhao, J.; Li, P.-F.; Xu, Y. Sustainable Disposal of Seawater Brine by Novel Hybrid Electrodialysis System: Fine Utilization of Mixed Salts. *Water Res.* **2021**, *201*, No. 117335.
(40) León, T.; Abdullah Shah, S.; López, J.; Culcasi, A.; Jofre, L.; Cipollina, A.; Cortina, J. L.; Tamburini, A.; Micale, G. Electrodialysis with Bipolar Membranes for the Generation of NaOH and HCl Solutions from Brines: An Inter-Laboratory Evaluation of Thin and Ultrathin Non-Woven Cloth-Based Ion-Exchange Membranes. *Membranes* **2022**, *12*, No. 1204, DOI: 10.3390/membranes12121204.

https://doi.org/10.1021/acs.energyfuels.4c00865
Energy Fuels 2024, 38, 15812−15822